Spacetime symmetry and mass of a lepton

2008 J. Phys. A: Math. Theor. 41 304033

(http://iopscience.iop.org/1751-8121/41/30/304033)

IOP PUBLISHING JOURNAL OF PHYSICS A: MATHEMATICAL AND THEORETICAL

J. Phys. A: Math. Theor. **41** (2008) 304033 (20pp) doi:10.1088/1751-8113/41/30/304033

Spacetime symmetry and mass of a lepton

Irina Dymnikova

Department of Mathematics and Computer Science, University of Warmia and Mazury, Żołnierska 14, 10-561 Olsztyn, Poland
and
AF Ioffe Physico-Technical Institute, Politekhnicheskaja 26, St Petersburg 194021, Russia

E-mail: irina@matman.uwm.edu.pl

Received 24 October 2007, in final form 20 January 2008
Published 15 July 2008
Online at stacks.iop.org/JPhysA/41/304033

Abstract

The Einstein equations admit the class of regular solutions generated by stress-energy tensors representing vacuum with the reduced symmetry as compared with the maximally symmetric de Sitter vacuum. In the spherically symmetric case they describe, in particular, gravitational vacuum solitons with the de Sitter center whose mass is related to the de Sitter vacuum trapped inside and smooth breaking of spacetime symmetry from the de Sitter group in the origin to the Poincaré group at infinity. In nonlinear electrodynamics coupled to gravity and satisfying the weak energy condition, an electrovacuum soliton has an obligatory de Sitter center where the electric field vanishes while the energy density of the electromagnetic vacuum achieves its maximal finite value which gives a natural cutoff on self-energy. By the Gürses–Gürsey algorithm based on the Trautman–Newman technique it is transformed into a spinning electrovacuum soliton asymptotically Kerr–Newman for a distant observer, with the gyromagnetic ratio $g = 2$. The de Sitter center becomes the de Sitter equatorial disk which has properties of a perfect conductor and ideal diamagnetic. The interior de Sitter vacuum disk displays superconducting behavior within a single spinning particle. This behavior is generic for the class of spinning electrovacuum solitons. The de Sitter vacuum supplies a particle with the finite electromagnetic mass related to breaking of spacetime symmetry.

PACS numbers: 04.70.Bw, 04.20.Dw

(Some figures in this article are in colour only in the electronic version)

1. Introduction

Approach. We report here the results obtained in the frame of a model-independent analysis of relevant field equations. Such an approach allows one to reveal the basic information contained

in the equations and thus generic behavior implied by them. For the case of electromagnetically interacting objects the relevant equations come from nonlinear electrodynamics coupled to gravity.

The Einstein equations

$$G^{\mu}_{\nu} = R^{\mu}_{\nu} - \tfrac{1}{2}R\delta^{\mu}_{\nu} = -\kappa\langle T^{\mu}_{\nu}\rangle, \qquad \kappa = 8\pi G \tag{1.1}$$

tell us that there exists the class of regular solutions with the de Sitter center, specified by [1, 2]

$$T^0_0 = T^1_1, \tag{1.2}$$

which represents an anisotropic vacuum dark fluid [3], and describes spherical objects whose masses are related to de Sitter vacuum and (smooth) breaking of spacetime symmetry from the de Sitter group in the origin to the Poincaré group at infinity [4, 5].

In nonlinear electrodynamics coupled to gravity solutions of this class represent spherical electrovacuum solitons (the only contribution to a stress-energy tensor comes from a source-free electromagnetic field which always satisfies (1.2)). By the Gürses–Gürsey algorithm it gives rise to the class of regular axially symmetric solutions, asymptotically Kerr–Newman for a distant observer, describing spinning charged objects ($s = \hbar/2$, $g = 2$) with the finite positive electromagnetic mass related to breaking of spacetime symmetry and to interior rotating superconducting de Sitter vacuum [6].

Maximally symmetric de Sitter vacuum is associated with the Einstein cosmological term [7, 8]

$$\langle T^{\nu}_{\mu}\rangle = \langle\rho_{\rm vac}\rangle\delta^{\nu}_{\mu} = \kappa^{-1}\Lambda\delta^{\nu}_{\mu} \tag{1.3}$$

and satisfies the equation of state

$$p = -\rho. \tag{1.4}$$

From the Einstein equations (more precisely from the contracted Bianchi identities) it follows

$$G^{\mu}_{\nu;\mu} = 0 \Rightarrow \langle\rho_{\rm vac}\rangle = \text{const}. \tag{1.5}$$

The de Sitter vacuum was identified as a vacuum by the algebraic structure of its stress-energy tensor: all eigenvalues are equal. As a result it has an infinite set of co-moving reference frames which makes impossible to fix a velocity with respect to it [7].

A vacuum with a reduced symmetry. The symmetry of a vacuum stress-energy tensor (1.3) can be reduced keeping its vacuum identity, i.e., invariance under Lorentz boosts in one (or two) spacelike directions ([3] and references therein)

$$p_k = -\rho. \tag{1.6}$$

A stress-energy tensor satisfying (1.6), is invariant under Lorentz boosts in the kth direction(s), so that one cannot single out a preferred co-moving reference frame and thus determine the velocity with respect to a medium specified by (1.6)—which is the intrinsic property of a vacuum [9].

A vacuum defined by the symmetry of its stress-energy tensor, must be evidently anisotropic (except the maximally symmetric de Sitter vacuum (1.3)).

Variability of a vacuum density $\rho_{\rm vac}$ for a vacuum with the reduced symmetry follows from the Einstein equations: $G^{\mu}_{\nu;\mu} = 0$ leads to $\rho_{\rm vac} \neq$ const and to the equation of state for the case of a particular symmetry.

In the spherically symmetric case, anisotropic spherically symmetric vacuum is defined by [1, 2, 4]

$$T^t_t = T^r_r, \qquad T^{\theta}_{\theta} = T^{\phi}_{\phi}. \tag{1.7}$$

A regular vacuum stress-energy tensor (1.7) describes a *smooth continuous* de Sitter–Schwarzschild transition relating de Sitter vacuum $T^\mu_\nu = \rho_{\rm vac}\delta^\mu_\nu$ in the center with the Minkowski vacuum $T^\mu_\nu = 0$ at infinity

$$T^\mu_\nu{}_{\rm deSitter} \quad \longleftarrow \quad T^\mu_\nu \quad \longrightarrow T^\mu_\nu{}_{\rm Minkowski}.$$

It satisfies the equation of state for anisotropic perfect fluid with continuous density and pressures [1]

$$p_r = -\rho, \qquad p_\perp = -\rho - \frac{r}{2}\rho'. \tag{1.8}$$

Globally regular spherically symmetric spacetime with de Sitter center [5] (for a recent review [3, 10]) represents, dependently on the choice of observers (coordinate mapping) distributed or localized vacuum energy: regular vacuum dominated cosmologies [11–13], vacuum nonsingular black holes [1, 14] (for review [10, 15]) and self-gravitating vacuum compact objects without horizons [16, 17], called G-lumps [4] which are stable for a wide class of density profiles $\rho(r)$ [3].

The existence of the class of solutions with de Sitter center follows from the requirements of regularity of density, finiteness of the mass and the weak energy condition for $T_{\mu\nu}$. Masses of objects are generically related to smooth breaking of spacetime symmetry from the de Sitter group in the origin, and to de Sitter vacuum trapped inside [2, 4, 17–21].

Another approach involving an interior de Sitter vacuum is based on direct matching of de Sitter interior to the Schwarzschild exterior via thin transitional shell where the metric typically suffers from discontinuities [22–31].

Contained in general relativity class of solutions specified by (1.6) which describe time dependent and spatially inhomogeneous vacuum energy, represents a model-independent unified description (based on a spacetime symmetry) of dark ingredients in the universe by a vacuum dark fluid which can both be distributed and form gravitationally bound compact vacuum objects [3].

In the context of a vacuum fluid unification, relation dark energy–dark matter (not necessary dark) may appear quite nontrivial. In nonlinear electrodynamics coupled to gravity spherically symmetric electrovacuum soliton must have obligatory de Sitter center [32] which for a spinning particle transforms into rotating de Sitter vacuum disk displaying superconducting behavior within a single spinning particle [6].

This paper is organized as follows. In section 2, we outline the basic features of regular spacetimes with de Sitter center. In section 3, we present spinning superconducting electrovacuum soliton. In section 4, we outline estimates confronting electrovacuum soliton with experiments, and in section 5 we summarize the results.

2. Spherically symmetric spacetime with de Sitter center

The existence of the globally regular spherically symmetric geometries follows from the following requirements [4]:

(a) Regularity of density $\rho(r)$,
(b) Finiteness of the mass $m = 4\pi\int_0^\infty \rho(r)r^2\,{\rm d}r$,
(c1) Dominant energy condition for $T_{\mu\nu}$ which implies $\rho \geqslant 0$; $\rho + p_k \geqslant 0$ for any observer, and $p_k \leqslant \rho$ for each principal pressure (which in turn implies speed of sound never exceeding speed of light, $v_s \leqslant c$).

The second option is

(c2) Weak energy condition for $T_{\mu\nu}$ which is contained in the dominant energy condition and requires only $\rho \geqslant 0$; $\rho + p_k \geqslant 0$ for any observer. Two cases (c) differ in that the case (c2) admits smooth changes in topology of spacelike hypersurfaces ([10] and references therein).

Conditions (a)–(c) lead to the existence of the family of geometries with the regular center [4]. The famous example from this family is boson stars [33, 34] which are regular configurations without horizons generated by self-gravitating massive complex scalar field whose stress-energy tensor is essentially anisotropic.

Class of geometries with the de Sitter center contained in this family is specified by (1.7). A static spherically symmetric line element is given by [1, 4]

$$ds^2 = g(r)\,dt^2 - \frac{dr^2}{g(r)} - r^2\,d\Omega^2, \tag{2.1}$$

where $d\Omega^2$ is the metric on a unit 2-sphere, and the metric function $g(r)$ is given by

$$g(r) = 1 - \frac{R_g(r)}{r}, \qquad R_g(r) = 2G\mathcal{M}(r), \tag{2.2}$$

with the mass function

$$\mathcal{M}(r) = 4\pi \int_0^r \rho(x)x^2\,dx. \tag{2.3}$$

The metrics are asymptotically Schwarzschild at large r and asymptotically de Sitter as $r \to 0$

$$1 - \frac{\Lambda}{3}r^2 \quad \leftarrow \quad g(r) \quad \rightarrow \quad 1 - \frac{2Gm}{r},$$

where the mass parameter m (gravitational mass) is given by

$$m = 4\pi \int_0^\infty \rho(r)r^2\,dr \tag{2.4}$$

and the cosmological constant Λ is related to the density of the de Sitter vacuum ρ_0 by

$$\Lambda = \kappa\rho_0. \tag{2.5}$$

The weak energy condition leads to the monotonic decrease of a density profile, $\rho' \leqslant 0$, and the requirement of regularity leads to the obligatory de Sitter center [4, 5, 32]. Spacetime can have not more than two Killing horizons, a black hole horizon r_+ and an internal horizon r_- related to appearance of de Sitter vacuum instead of a Schwarzschild singularity [4].

In the coordinates of a distant observer at rest (e.g., r, t in (2.1)) the class of solutions specified by (1.2), describes compact objects dominated by anisotropic vacuum dark fluid (the word 'dark' refers to their interiors), a black hole for $m \geqslant m_{\rm cr}$, and self-gravitating vacuum soliton, G-lump for $m < m_{\rm cr}$ [16, 17, 4].

Three compact vacuum configurations (a black hole, extreme black hole and G-lump) are shown in figure 1 plotted for the density profile [1]

$$\rho(r) = \rho_0\,e^{-r^3/r_0^2 r_g}, \qquad r_0^2 = 3/\kappa\rho_0, \qquad r_g = 2Gm, \tag{2.6}$$

which describes a smooth de Sitter–Schwarzschild transition in a simple semiclassical model for vacuum polarization in the spherically symmetric gravitational field ([16] and references therein). In this case the critical mass is $m_{\rm cr} \simeq 0.3 m_{\rm Pl}\sqrt{\rho_{\rm Pl}/\rho_0}$.

Hawking temperature. Nonsingular vacuum black hole emits Hawking radiation from both black hole and internal horizons with the Gibbons–Hawking temperature $T_H = \hbar\Upsilon(2\pi kc)^{-1}$[35], where Υ is the surface gravity. The form of the temperature–mass diagram,

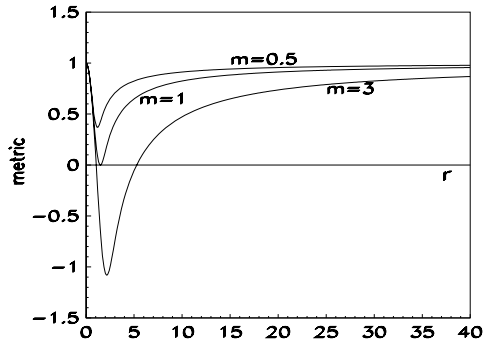

Figure 1. The metric function $g(r)$ for compact vacuum objects with de Sitter center. Mass m is normalized to $m_{\rm cr}$.

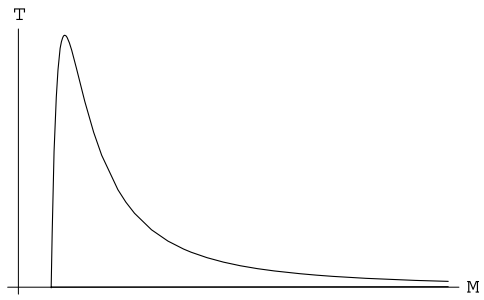

Figure 2. Typical behavior of the Hawking temperature for a regular vacuum black hole.

shown in figure 2, is generic for de Sitter–Schwarzschild geometry. The temperature on the BH T_+ horizon drops to zero as $m \to m_{\rm cr}$, while the Schwarzschild asymptotic requires $T_+ \to 0$ as $m \to \infty$. As a result the temperature–mass curve has a maximum between $m_{\rm cr}$ and $m \to \infty$, where a specific heat is broken and changes its sign testifying for a second-order phase transition in the course of Hawking evaporation and suggesting restoration of spacetime symmetry to the de Sitter group in the origin [17].

For the density profile (2.6)

$$T_+ = \frac{\hbar c}{4\pi k r_0}\left[\frac{r_0}{r_+} - \frac{3r_+}{r_0}\left(1 - \frac{r_+}{r_g}\right)\right]. \tag{2.7}$$

Temperature achieves its maximal value $T_{\rm max}$ at the value of mass parameter m_{tr}. They are given by

$$m_{tr} \simeq 0.4 m_{\rm Pl}\sqrt{\rho_{\rm Pl}/\rho_0}, \qquad T_{\rm max} \simeq 0.2 T_{\rm Pl}\sqrt{\rho_{\rm Pl}/\rho_0}.$$

For the scale of symmetry restoration $M \sim 10^{15}$ GeV,

$$m_{\rm cr} \simeq 0.3 \times 10^{11}\ {\rm GeV}, \qquad m_{tr} \simeq 0.2 \times 10^{11}\ {\rm GeV}$$

$$T_{\rm max} \simeq 0.2 \times 10^{11}{\rm GeV}. \tag{2.8}$$

In the course of Hawking evaporation a black hole evolves toward a G-lump [4, 16, 17], particlelike or starlike dependently on mass and the scale ρ_0 of interior de Sitter vacuum, bound

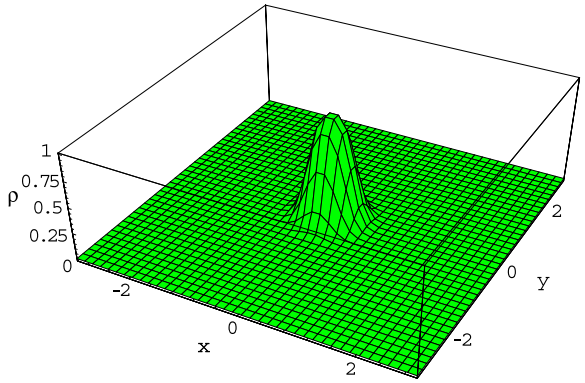

Figure 3. G-lump in the case $r_g = 0.1r_0$ ($m \simeq 0.06m_{\rm crit}$).

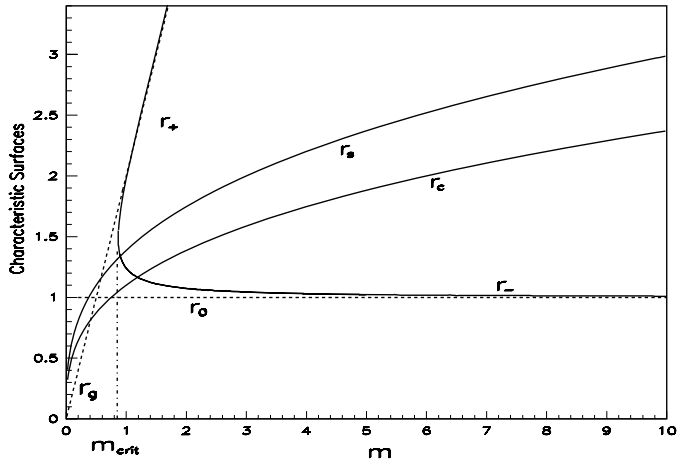

Figure 4. Horizons and surfaces $r = r_s$ and $r = r_c$.

by their own gravity balanced at the zero-gravity surface where the strong energy condition ($\rho + \sum p_k \geqslant 0$) is violated and gravitational attraction becomes gravitational repulsion. G-lump is plotted in figure 3 for the density profile (2.6).

A zero-gravity surface $r = r_c$ exists for any geometry with a de Sitter center and is defined by $p_\perp(r) = 0$ [2, 16].

For configurations satisfying the weak energy condition, there exist two additional characteristic surfaces: surfaces of zero 4- and 3-curvature. The surface of zero scalar 4-curvature $r = r_s$ ($R(r_s) = 0$) represents the characteristic curvature size in the de Sitter–Schwarzschild geometry in the case (c2). Surfaces $r = r_c$ and $r = r_s$ are depicted in figure 4 together with horizons. For the density profile (2.6) the characteristic size r_s is given by [16]

$$r_s = \left(\frac{4}{3}r_0^2 r_g\right)^{1/3} = \left(\frac{m}{\pi\rho_0}\right)^{1/3}. \tag{2.9}$$

Cosmological term as a source of mass. Vacuum with the reduced symmetry can be associated with a time-evolving spatially inhomogeneous cosmological term [2]

$$\Lambda_k^i = \kappa T_k^i. \tag{2.10}$$

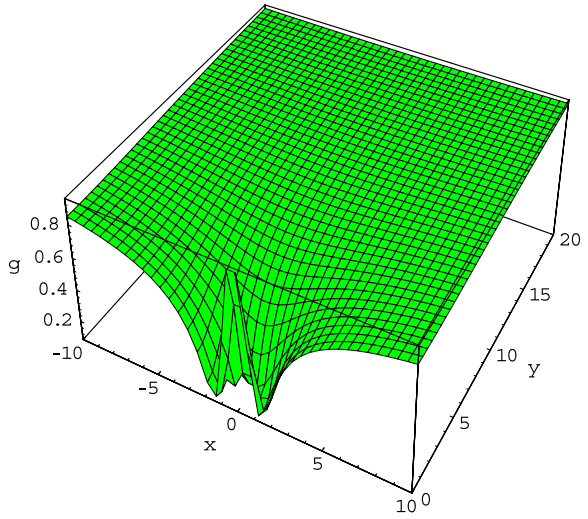

Figure 5. The gravitational potential $g(r)$ for the case of G-lump with the mass a little bit less than $m_{\rm cr}$.

The Einstein equation with the cosmological term is generalized to [2, 4]

$$G^\mu_\nu + \Lambda\delta^\mu_\nu = 0 \longrightarrow G^\mu_\nu + \Lambda^\mu_\nu = 0,$$

so that the Einstein cosmological constant Λ becomes time-evolving and space-inhomogeneous component $\Lambda^t_t = \kappa T^t_t = \kappa\rho$ of the variable cosmological term (2.10).

The mass (2.4) is defined thus, in the asymptotically flat case, by [4]

$$m = \frac{1}{2G}\int_0^\infty \Lambda^t_t(r) r^2\,{\rm d}r \tag{2.11}$$

and is generically related to an interior de Sitter vacuum.

This picture conforms with the basic idea of the Higgs mechanism for generation of mass via spontaneous breaking of symmetry of a scalar field vacuum from a false vacuum to a true vacuum state. In both cases de Sitter vacuum is involved and vacuum symmetry is broken.

The difference is that the gravitational potential $g(r)$ (shown in figure 5) is generic, and the de Sitter vacuum supplies a particle with mass via smooth breaking of spacetime symmetry from the de Sitter group in its center to the Poincaré group at its infinity in the asymptotically flat spacetime [4]

$$\text{de Sitter group}\ \ 0 \longleftarrow r \longrightarrow \infty \quad \text{Poincare group}$$

or to the de Sitter group with another value of vacuum density in the asymptotically de Sitter spacetime with $\lambda < \Lambda$ ([21] and references therein).

3. Spinning superconducting electrovacuum soliton

3.1. Kerr–Newman spacetime

The Kerr–Newman line element is given by [36]

$${\rm d}s^2 = {\rm d}t^2 - \frac{(2mr - e^2)}{\Sigma}({\rm d}t - a\sin^2\theta\,{\rm d}\phi)^2 - \frac{\Sigma}{\Delta}{\rm d}r^2 - \Sigma\,{\rm d}\theta^2 - (r^2 + a^2)\sin^2\theta\,{\rm d}\phi^2 \tag{3.1}$$

$$\Sigma = r^2 + a^2\cos^2\theta, \qquad \Delta = r^2 - 2mr + a^2 + e^2. \tag{3.2}$$

The associated electromagnetic potential is

$$A_i = -\frac{er}{\Sigma}[1; 0, 0, -a\sin^2\theta]. \tag{3.3}$$

The parameter m represents the mass and e the charge in the limit of large r. The parameter a is identified as the specific angular momentum ([37] and references therein).

Since the parameter a couples with the mass to give the angular momentum ma, and with the charge to give an asymptotic magnetic dipole momentum ea, there is no freedom of variation of the gyromagnetic ratio e/m, which appears exactly the same as predicted by the Dirac equation for a relativistic quantum spinning particle. Therefore one can choose the parameters in (3.1)–(3.3) in such a way that they correspond to the electron parameters, $m \approx 10^{-22}$; $ma = 1/2$; $e^2 \approx 1/137$ in the units $\hbar = c = G = 1$. The resulting characteristic length scale is the Compton radius [37].

The Kerr–Newman geometry belongs to the Kerr family of solutions of the source-free Maxwell–Einstein equations, the only contribution to the stress-energy tensor comes from a source-free electromagnetic field [37].

In the Kerr family solutions the surfaces $r = \text{const}$ are confocal oblate ellipsoids of revolution whose principal axis coincide with the coordinate axes. They are described by (see, e.g., [38])

$$r^4 - (x^2 + y^2 + z^2 - a^2)r^2 - a^2z^2 = 0. \tag{3.4}$$

For $r = 0$ the ellipsoids degenerate to the disk

$$x^2 + y^2 \leqslant a^2, \qquad z = 0 \tag{3.5}$$

encircled by the ring

$$x^2 + y^2 = a^2, \qquad z = 0 \tag{3.6}$$

and the singularity along this ring is the only singularity of the Kerr and the Kerr–Newman spacetime called the Kerr ring singularity (see [38] for systematic description).

The main disaster of the Kerr–Newman geometry discovered by Carter is nontrivial causality violation in the case of a charged spinning particle [37]

$$a^2 + e^2 > m^2. \tag{3.7}$$

In this case, there are no Killing horizons, the manifold is geodesically complete (except for geodesics which reach the singularity at $\Sigma = 0$), and any point can be connected to any other point by both a future and a past directed timelike curve. The condition of the causality violation

$$r^2 + a^2 + \Sigma^{-1}(2mr - e^2)a^2\sin^2\theta < 0 \tag{3.8}$$

is satisfied in the vicinity of the Kerr disk where the vector $\partial/\partial\phi$ is timelike, but closed timelike curves entering the region (3.8) can extend over the whole space and cannot be removed by taking a covering space [37].

The Kerr–Newman solution represents the exterior fields of rotating charged bodies. The question of a physically natural interior material source for these fields is the most intriguing question, because this geometry which implies the gyromagnetic ratio $g = 2$ favored by particle physics, encounters gross causality problem just in the case of a particle.

The source models for the Kerr–Newman interior can be roughly divided into disklike [39–43], shelllike [44–46], baglike [47–53] and stringlike ([54] and references therein).

Below we outline the results obtained in [6, 32]. In nonlinear electrodynamics coupled to general relativity and satisfying the weak energy condition, a regular spherically symmetric electrically charged structure has an obligatory de Sitter center. By the Gürses–Gürsey algorithm based on the Newman–Trautman technique it is transformed into a spinning electrovacuum structure asymptotically Kerr–Newman for a distant observer, with the gyromagnetic ratio $g = 2$.

3.2. Basic equations of nonlinear electrodynamics coupled to gravity

In the nonlinear electrodynamics minimally coupled to gravity, the action is given by

$$S = \frac{1}{16\pi G}\int \mathrm{d}^4x\sqrt{-g}[R - \mathcal{L}(F)], \tag{3.9}$$

where R is the scalar curvature, and $F = F_{\mu\nu}F^{\mu\nu}$ is the electromagnetic invariant, with $F_{\mu\nu} = \partial_\mu A_\nu - \partial_\nu A_\mu$. The gauge-invariant electromagnetic Lagrangian $\mathcal{L}(F)$ is an arbitrary function of F which should have the Maxwell limit, $\mathcal{L} \to F$, $\mathcal{L}_F \to 1$ in the weak field regime.

The dynamic equations read

$$\nabla_\mu(\mathcal{L}_F F^{\mu\nu}) = 0, \tag{3.10}$$

where $\mathcal{L}_F = \mathrm{d}\mathcal{L}/\mathrm{d}F$, and the contracted Bianchi identities give

$$\nabla_\mu {}^*F^{\mu\nu} = 0. \tag{3.11}$$

An asterisk denotes the Hodge dual defined by [9]

$${}^*F^{\mu\nu} = \tfrac{1}{2}\eta^{\mu\nu\alpha\beta}F_{\alpha\beta}, \qquad {}^*F_{\mu\nu} = \tfrac{1}{2}\eta_{\mu\nu\alpha\beta}F^{\alpha\beta} \tag{3.12}$$

and the totally antisymmetric unit tensor is chosen in such a way that $\eta_{0123} = \sqrt{-g}$.

In terms of the field vectors defined as

$$\mathbf{E} = \{F_{\alpha 0}\}, \qquad \mathbf{D} = \{\mathcal{L}_F F^{0\alpha}\}, \qquad \mathbf{B} = \{{}^*F^{\alpha 0}\}, \qquad \mathbf{H} = \{\mathcal{L}_F {}^*F_{0\alpha}\} \tag{3.13}$$

the field equations (3.10) and (3.11) take, respectively, the conventional form of the Maxwell equations

$$\begin{aligned} &\nabla\mathbf{D} = 0, \qquad &&\nabla\times\mathbf{H} = \frac{\partial\mathbf{D}}{\partial t},\\ &\nabla\mathbf{B} = 0, \qquad &&\nabla\times\mathbf{E} = -\frac{\partial\mathbf{B}}{\partial t}. \end{aligned} \tag{3.14}$$

The stress-energy tensor of a nonlinear electromagnetic field is calculated in the standard way [9] which gives

$$\kappa T^\mu_\nu = -2\mathcal{L}_F F_{\nu\alpha}F^{\mu\alpha} + \tfrac{1}{2}\delta^\mu_\nu\mathcal{L}. \tag{3.15}$$

3.3. Spherically symmetric electrovacuum soliton

The stress-energy tensor of the spherically symmetric electromagnetic field with an arbitrary gauge-invariant Lagrangian $\mathcal{L}(F)$, has the algebraic structure (1.2).

For the class of regular spherically symmetric geometries with the symmetry of a source term given by (1.2), the weak energy condition leads inevitably to de Sitter asymptotic at approaching a regular center [4].

Symmetry of a source term leads to the metric (2.1) which is asymptotically Reissner–Nordström in the weak field limit as $r \to \infty$, with the electromagnetic mass

$$m = 4\pi\int_0^\infty \rho_{\mathrm{EM}}(r)r^2\,\mathrm{d}r. \tag{3.16}$$

In the spherically symmetric case the only essential components of $F_{\mu\nu}$ are the radial electric field $F_{01} = E(r)$ and the radial magnetic field $F_{23} = -F_{32}$.

For an electrically charged structure, the first dynamical equation (3.10) yields

$$F^{01} = \frac{e}{\mathcal{L}_F r^2}, \tag{3.17}$$

where e is a constant of integration identified as an electric charge by asymptotic behavior in the weak field limit.

The field invariant is given by

$$F = 2F_{01}F^{01} = -\frac{2e^2}{\mathcal{L}_F^2 r^4}. \tag{3.18}$$

In the considered case $F = -2E^2$ with $E = e(\mathcal{L}_F r^2)^{-1}$.

The equation of state relating density with the radial pressure and tangential pressure is given by (1.8). With taking into account (3.15) it gives [32]

$$\kappa(p_\perp + \rho) = -F\mathcal{L}_F. \tag{3.19}$$

In the de Sitter center the left-hand side of (3.19) vanishes.

From (3.18) and (3.19) we get

$$\mathcal{L}_F = \frac{2e^2}{\kappa(p_\perp + \rho)r^4} \tag{3.20}$$

and

$$F = -\frac{\kappa^2(p_\perp + \rho)^2 r^4}{2e^2}. \tag{3.21}$$

The invariant F vanishes as $r \to 0$, so that the electric field vanishes in the center. Since F vanishes at both zero and infinity where it should follow the Maxwell weak field limit, F must have a minimum in between where an electric field strength has an extremum [32, 55].

The Lagrangian derivative $\mathcal{L}_F$ goes to infinity as $r \to 0$, so that a regular electrically charged structure is not compatible with the Maxwell weak field limit, $\mathcal{L} \to F$, $F \to 0$, $\mathcal{L}_F \to 1$, at the center ([32, 55] and references therein).

On the other hand, the weak energy condition requires $\rho' \leqslant 0$. Then ρ is maximal at the de Sitter center, and one cannot expect validity of the weak field limit in the region of maximal energy density of the field [32].

The Lagrangian $\mathcal{L}(F) \to 2\rho_0$ as $r \to 0$, by (3.19) and (3.15), so that Lagrangian is positive and takes its maximal value at the center which testifies that the limiting density as $r \to 0$ is of electromagnetic origin.

In the de Sitter center of an electrovacuum soliton, electric field F goes to zero, while the energy density of the electromagnetic field T_0^0 achieves its maximal value. The T_0^0 component of electromagnetic stress-energy tensor does not vanish (neither diverges) as $r \to 0$ and provides an effective cutoff on self-interaction by relating it, through Einstein equations, with cosmological constant Λ corresponding to the energy density of an electromagnetic vacuum in the center of a soliton [32].

The weak energy condition, $\rho + p_\perp \geqslant 0$, leads to $-F\mathcal{L}_F \geqslant 0$. It gives $\mathcal{L}_F \geqslant 0$. Since $\mathcal{L}(F)$ is the monotonic function of the invariant F which evolves from zero at the center to zero at infinity with a minimum in between, Lagrangian has two branches [32, 55], in other words, there are two Lagrangians here, one for the interior region (from the center to the extremum of the electric field tension), another for the exterior (asymptotically Maxwellian) region.

The strong energy condition for electrically charged configurations reads $2p_\perp = -\mathcal{L} \geqslant 0$. It is violated at the surface of zero gravity where $\mathcal{L} = 0$. The surface of zero gravity there exists in any electrically charged electrovacuum soliton.

3.4. Spinning electrovacuum soliton

Gürses and Gürsey have shown that spherically symmetric metrics of the Kerr–Schild class [56] can be transformed, by the complex Trautman–Newman translations, to spinning metrics [57]

$$ds^2 = \frac{\Sigma - 2f}{\Sigma}\,dt^2 + \frac{4af\sin^2\theta}{\Sigma}\,dt\,d\phi - \frac{\Sigma}{\Delta}\,dr^2 - \Sigma\,d\theta^2 - \left(r^2 + a^2 + \frac{2fa^2\sin^2\theta}{\Sigma}\right)\sin^2\theta\,d\phi^2, \tag{3.22}$$

where now

$$\Delta = r^2 + a^2 - 2f(r). \tag{3.23}$$

The function $f(r)$ comes from a spherically symmetric solution. In the rotating case the surfaces of constant r are confocal ellipsoids given by (3.4).

The eigenvalues of $T_{\mu\nu}$ are its components ρ, $p_\perp$ and $p_r = -\rho$ in the co-rotating references frame where each of ellipsoidal layers $r = \text{const}$ rotates with the angular velocity $\omega(r) = a/(r^2 + a^2)$ [53].

They are related to the function $f(r)$ in (3.22) by

$$\kappa\rho(r) = 2\frac{(f'r - f)}{\Sigma^2}, \qquad \kappa p_\perp = \frac{2(f'r - f) - f''\Sigma}{\Sigma^2}. \tag{3.24}$$

Static spherically symmetric solutions of the Einstein equations satisfying condition (1.2) belong to the Kerr–Schild class [53, 58]. By the Gürses–Gürsey algorithm, a regular non-rotating electrovacuum solution can be transformed into a regular spinning solution with the gyromagnetic ratio $g = 2$ [6].

The function $f(r)$ which comes to (3.22) from nonlinear electrodynamics coupled to gravity is given by

$$f(r) = G\mathcal{M}(r)r, \tag{3.25}$$

where the mass function $\mathcal{M}(r)$ defined by (2.3) is

$$\mathcal{M}(r) = \int_0^r \tilde{\rho}(x)x^2\,dx \tag{3.26}$$

and $\tilde{\rho}(r)$ is the spherically symmetric density profile responsible for the function $f(r)$ in (3.22).

For a spherically symmetric solution satisfying the weak energy condition, the function $f(r)$ is everywhere positive. For $r \to 0$ it approaches the de Sitter asymptotic

$$2f(r) = \frac{r^4}{r_0^2}, \qquad r_0^2 = \frac{3}{\Lambda} = \frac{3}{8\pi G\tilde{\rho}_0} \tag{3.27}$$

and then monotonically increases to the Kerr–Newman asymptotic for large r [6]

$$f_{de\,S} = \frac{4\pi\tilde{\rho}_0}{3}r^4 \longleftarrow f(r) \longrightarrow f_{KN} = mr - \frac{e^2}{2},$$

where $m = \mathcal{M}(r \to \infty)$ is the finite positive electromagnetic mass given by (3.16) with $\rho_{\rm EM} = \tilde{\rho}$.

Non-negativity of $f(r)$ guarantees that the condition of the causality violation (3.8) is never satisfied.

In the equatorial plane

$$\frac{2f(r)}{\Sigma} = \frac{r^2}{r_0^2}, \tag{3.28}$$

so that the equatorial disk $r = 0$ is totally (together with the ring) intrinsically flat.

But Λ is nonzero throughout the disk.

The original non-rotating metrics are asymptotically de Sitter as $r \to 0$ which is asymptotically flat but with nonzero Λ. Rotation transforms the point $r = 0$ into the disk (3.5). The metric (3.22) in this limit takes the form

$$ds^2 = \left(\frac{r^2}{r_0^2} - 1\right) dt^2 + \frac{r^2}{\Delta} dr^2 + r^2 d\theta - \frac{r^2}{r_0^2} 2a\, dt\, d\phi + \left(r^2 + a^2 + \frac{r^2}{r_0^2}\right) d\phi^2. \tag{3.29}$$

The asymptotic (3.29) represents the rotating de Sitter vacuum with Λ spread over the equatorial disk (3.5).

The equation of state in the co-rotating frame

$$p_r(r,\theta) = -\rho(r,\theta), \qquad p_\perp(r,\theta) = -\rho - \frac{\Sigma}{2r}\frac{\partial\rho(r,\theta)}{\partial r} \tag{3.30}$$

relates the eigenvalues of the stress-energy tensor (3.24)

$$\rho(r,\theta) = \frac{r^4}{\Sigma^2}\tilde{\rho}(r) \qquad p_\perp = \left(\frac{r^4}{\Sigma^2} - \frac{2r^2}{\Sigma}\right)\tilde{\rho}(r) - \frac{r^3}{2\Sigma}\tilde{\rho}'(r). \tag{3.31}$$

The prime denotes the differentiation with respect to r.

At the ellipsoidal layers

$$\frac{r^2}{\Sigma} = \frac{(x^2+y^2+z^2-a^2)r^2 + a^2z^2}{(x^2+y^2+z^2-a^2)r^2 + 2a^2z^2}. \tag{3.32}$$

In the limit $z \to 0$ it goes to the unity identically in the whole equatorial plane.

Taking the limit $z \to 0$ in (3.32) we find that

$$\rho(r,\theta) = \tilde{\rho}(r), \qquad p_\perp + \rho = -\frac{r^3}{2\Sigma}\tilde{\rho}'(r) \tag{3.33}$$

identically in the whole equatorial plane including the disk, the ring and the origin. For spherically symmetric solutions regularity requires $r\tilde{\rho}'(r) \to 0$ as $r \to 0$ [32]. With taking into account (3.32) we find that on the disk

$$r \to 0, \qquad z \to 0, \qquad r^2/\Sigma \to 1 \tag{3.34}$$

the equation of state becomes

$$p_r = p_\perp = -\rho \tag{3.35}$$

and represents rotating de Sitter vacuum in the co-rotating frame.

At the de Sitter equatorial disk (3.34)–(3.35)

$$\kappa\rho(r,\theta) = \Lambda. \tag{3.36}$$

Nonzero field components compatible with the axial symmetry are F_{01}, F_{02}, F_{13}, F_{23}.

The field intensities are given by

$$\begin{aligned} &E_r = F_{10}, \qquad E_\theta = F_{20}, \qquad H_r = \mathcal{L}_F\sqrt{-g}F^{23}, \qquad H_\theta = \mathcal{L}_F\sqrt{-g}F^{31}, \\ &D^r = \mathcal{L}_F F^{01}, \qquad D^\theta = \mathcal{L}_F F^{02}, \qquad \sqrt{-g}B^r = F_{23}, \qquad \sqrt{-g}B^\theta = F_{31}, \end{aligned} \tag{3.37}$$

where

$$\begin{aligned} &\Sigma F^{01} = (r^2+a^2)F_{10}, \qquad &&\Sigma\sin^2\theta F^{31} = F_{31}, \\ &\Sigma F^{02} = F_{20}, &&\Sigma(r^2+a^2)\sin^2\theta F^{23} = F_{23}. \end{aligned} \tag{3.38}$$

As follows from (3.37)–(3.38), the electric field intensity $\mathbf{E}$ is connected with the electric induction $\mathbf{D}$ as

$$D_\alpha = \epsilon_{\alpha\beta}E_\beta, \tag{3.39}$$

where $\epsilon_{\alpha\beta}$ is the tensor of the dielectric permeability, so that nonlinear electromagnetic field in geometry (3.22) behaves like anisotropic dielectric medium. Equipotential field surfaces are the oblate ellipsoids (3.4). Their symmetry gives two independent eigenvalues of $\epsilon_{\alpha\beta}$:

$$\epsilon_r = \frac{(r^2+a^2)}{\Delta}\mathcal{L}_F, \qquad \epsilon_\theta = \mathcal{L}_F. \tag{3.40}$$

In the de Sitter region dielectric medium becomes isotropic with $\epsilon_r = \epsilon_\theta = \mathcal{L}_F$.

The magnetic field intensity **H** is related with the magnetic induction **B** by

$$B_\alpha = \mu_{\alpha\beta} H_\beta, \tag{3.41}$$

where $\mu_{\alpha\beta}$ is the tensor of magnetic permeability whose independent eigenvalues are

$$\mu_r = \frac{(r^2+a^2)}{\Delta}\frac{1}{\mathcal{L}_F}, \qquad \mu_\theta = \frac{1}{\mathcal{L}_F}. \tag{3.42}$$

In the de Sitter region $\mu_r = \mu_\theta = {\mathcal{L}_F}^{-1}$.

The dynamic equations (3.10) yield

$$\begin{aligned} \mathcal{L}_F F_{10} &= \frac{e(r^2 - a^2\cos^2\theta)}{\Sigma^2}, \qquad \mathcal{L}_F F_{20} = -\frac{era^2\sin 2\theta}{\Sigma^2} \\ \mathcal{L}_F F_{31} &= \frac{ea(r^2 - a^2\cos^2\theta)}{\Sigma^2}, \qquad \mathcal{L}_F F_{23} = \frac{ear(r^2+a^2)\sin 2\theta}{\Sigma^2}. \end{aligned} \tag{3.43}$$

In the Kerr–Newman region $\mathcal{L}_F \to 1$ and the field components reduce to the Carter expressions [37].

The field invariant $F = F_{\mu\nu}F^{\mu\nu}$ takes the form

$$F = 2\left(\frac{F_{20}^2}{a^2\sin^2\theta} - F_{10}^2\right). \tag{3.44}$$

3.5. Elementary superconductivity

The equation of state in the co-rotating frame [6]

$$\kappa(p_\perp + \rho) = 2\left(\mathcal{L}_F F_{10}^2 + \mathcal{L}_F \frac{F_{20}^2}{a^2\sin^2\theta}\right) \tag{3.45}$$

allows one to investigate the behavior of the fields on the de Sitter vacuum disk, since geometry defines the behavior of the left-hand side there by equation (3.35).

Equations (3.43) give

$$\frac{F_{20}^2}{a^2\sin^2\theta} + F_{10}^2 = \frac{e^2}{\mathcal{L}_F^2\Sigma^2}. \tag{3.46}$$

Putting this in (3.45) we get

$$\kappa(p_\perp + \rho) = \frac{2e^2}{\mathcal{L}_F\Sigma^2}. \tag{3.47}$$

Equations (3.43) and (3.44) give the equation basic for study behavior of field configuration on the disk

$$\mathcal{L}_F^2 F = -\frac{2e^2}{\Sigma^2} + \frac{16e^2r^2a^2\cos^2\theta}{\Sigma^4}. \tag{3.48}$$

Equations (3.45)–(3.48) are valid everywhere.

In the second term of (3.48) we have

$$\frac{r^2a^2\cos^2\theta}{\Sigma^2}=\frac{r^2}{\Sigma}-\frac{r^4}{\Sigma^2}. \tag{3.49}$$

In the equatorial plane it vanishes by (3.32), as a result at the equatorial plane (3.48) reduces to

$$\mathcal{L}_F^2 F\Sigma^2=-2e^2. \tag{3.50}$$

Combining (3.50) valid in the equatorial plane with (3.47) valid everywhere, we get in the equatorial plane

$$\mathcal{L}_F F=-\kappa(p_\perp+\rho). \tag{3.51}$$

Equations (3.50) and (3.51) give in the equatorial plane

$$\mathcal{L}_F=\frac{2e^2}{\kappa\Sigma^2(p_\perp+\rho)},\qquad F=-\frac{\kappa^2(p_\perp+\rho)^2\Sigma^2}{2e^2}. \tag{3.52}$$

At the disk the field invariant F vanishes. The sign of $\mathcal{L}_F$ coincides with that of $(p_\perp+\rho)$ which is everywhere non-negative, because $\tilde{\rho}'$ is everywhere non-positive for the spherically symmetric solutions with de Sitter center.

Dielectric permeability $\mathcal{L}_F$ goes to infinity and magnetic permeability ${\mathcal{L}_F}^{-1}$ goes to zero. The de Sitter equatorial disk displays thus both perfect conductor and ideal diamagnetic behavior.

On the disk the left-hand side in (3.45) goes to zero, so that each component in the right-hand side vanishes

$$\mathcal{L}_F\frac{F_{20}^2}{a^2\sin^2\theta}=0,\qquad \mathcal{L}_F F_{10}^2=0. \tag{3.53}$$

It follows that

$$\frac{2e^2(B^r)^2}{\kappa(p_\perp+\rho)(r^2+a^2)^2}=0,\qquad \frac{2e^2(B^\theta)^2}{\kappa(p_\perp+\rho)a^2}=0, \tag{3.54}$$

hence both $(B^r)^2$ and $(B^\theta)^2$ should vanish at the disk faster than $(p_\perp+\rho)$, so that the magnetic induction $\mathbf{B}$ vanishes. The Meissner effect takes place for a single spinning soliton and occurs on its equatorial disk.

On the intrinsically flat disk (see equation (3.28)) we can apply the conventional definition of the surface current [59]

$$\mathbf{g}=\frac{1-\mu}{4\pi\mu}[\mathbf{nB}], \tag{3.55}$$

where $\mathbf{n}$ is the normal to the surface.

On the de Sitter disk both magnetic induction $\mathbf{B}$ and magnetic permeability ${\mathcal{L}_F}^{-1}$ go to zero independently.

Condition (3.55) relates the current density $\mathbf{g}$ to the magnetic induction inside a body and thus to the currents on its surface. In a non-superconductor $\int[\mathbf{nB}]\,\mathrm{d}\mathbf{f}=0$, so that the surface currents always balance, and the total current is zero. The transition to a superconducting state corresponds formally to the limits $\mathbf{B}\to 0$ and $\mu\to 0$. The right-hand side of (3.55) then becomes indeterminate, and there is no condition which would restrict the possible values of the current [59].

The currents flowing on the surface of de Sitter disk can be any and amount to a nonzero total value. It is important that a steady flow of current on a superconductor is possible even if no electric field is present [59].

From (3.44) and (3.45) it follows that on the disk $F=-4F_{10}^2$, so that both $E_r^2=F_{10}^2$ and $E_\theta^2=F_{20}^2$ vanish. The electric fields are zero at the disk, and superconducting currents can flow eternally.

4. Estimates

Nonlinear electrodynamics was proposed by Born and Infeld 70 years ago [60]. Today NED theories appear as low energy effective limits in certain models of string/M-theory (for review [61, 62]). Therefore the above results apply directly to the cases when relevant NED scale is much lower than the Planck scale.

Assuming that an extended particle dominated by electromagnetic interaction can be approached by nonlinear electrodynamics coupled to gravity, so that de Sitter vacuum is essentially involved in mass generation [4], we can test this by two preliminary estimates: mass-square difference for neutrino related to a gravito-electroweak scale where they get mass from a de Sitter vacuum [63, 64], and geometric size of a lepton [65] (for a recent review [66]).

4.1. Estimate of a gravito-electroweak unification scale from experimental data on neutrino

If in the interaction region where particles are created, the interaction vertex is gravito-electroweak, the gravity is involved essentially, and geometry around the vertex is not Minkowski anymore.

If density in the vertex is limited, mass of a particle is finite and some of conditions (c) holds, then geometry around the vertex can be de Sitter. If a false vacuum is somehow involved (for example via Higgs mechanism), then geometry in the interaction region is de Sitter.

If de Sitter group is the spacetime symmetry group induced around the gravito-electroweak vertex, then particles participating in the vertrex are described by the eigenstates of Casimir operators in the de Sitter geometry. Their further evolution in Minkowski background requires further symmetry change. As a result, in particular, the 'flavor' could emerge due to a change in symmetry group from de Sitter group around the vertex to the Poincaré group at infinity [63].

In the creation region, a particle is characterized by an eigenstate of the de Sitter Casimir invariants, $|I_1', I_2'\rangle$. I_1', I_2' are eigenvalues of the de Sitter Casimir operators I_1 and I_2 [67]. Here we need I_1 to study influence of de Sitter vacuum on a mass. It reads

$$I_1 = -\Pi_\mu \Pi^\mu - \frac{1}{2r_0^2} J_{\mu\nu} J^{\mu\nu}, \tag{4.1}$$

with

$$\Pi_\mu = \left(1 + \frac{r^2 - c^2t^2}{4r_0^2}\right) P_\mu + \frac{1}{2r_0^2} x^\nu J_{\mu\nu}. \tag{4.2}$$

The scale r_0 is characteristic de Sitter radius related to the vacuum density ρ_0 by

$$r_0^2 = \frac{3c^2}{8\pi G\rho_0}. \tag{4.3}$$

In the interaction region $r^2 - c^2t^2 \ll r_0^2$ [63], and the operator I_1 is approximated by

$$I_1 \approx -P_\mu P^\mu - \frac{1}{r_0^2}\left(\mathbf{J}^2 - \mathbf{K}^2\right), \tag{4.4}$$

where $J_{ij} = -J_{ji} = \epsilon_{ijk} J_k$ and $J_{i0} = -J_{0i} = -K_i$, with each of the i, j, k taking the values 1, 2, 3. The $\mathbf{J}$ are thus generators of Lorentz rotation and $\mathbf{K}$ are generators of Lorentz boosts

$$\mathbf{J} = \hbar\frac{\sigma}{2}, \qquad \mathbf{K} = -\mathrm{i}\hbar\frac{\sigma}{2} \tag{4.5}$$

for the right-handed fields, and

$$\mathbf{J} = \hbar\frac{\sigma}{2}, \qquad \mathbf{K} = +\mathrm{i}\hbar\frac{\sigma}{2} \tag{4.6}$$

for the left-handed fields. This gives

$$I_1 \approx - - P_\mu P^\mu - \frac{\hbar^2}{2r_0^2}\sigma^2. \tag{4.7}$$

Its eigenvalues are

$$I_1' = \mu^2 c^2 \pm \frac{\hbar^2}{2r_0^2}. \tag{4.8}$$

Suppressing I_2', when the state $|I_1'\rangle$ propagates in the Minkowski region, in terms of the first Poincare Casimir operator, $P_\mu P^\mu$, it appears as a linear superposition of two different mass eigenstates [63]

$$m_1^2 = \mu^2 + \frac{\hbar^2}{2c^2 r_0^2}, \qquad m_2^2 = \mu^2 - \frac{\hbar^2}{2c^2 r_0^2} \tag{4.9}$$

with equal weights. We see that the de Sitter symmetry in the gravito-electroweak vertex leads to an exact bi-maximal mixing for neutrinos. For $\hbar^2/(2r_0^2) > \mu^2 c^2$, m_2^2 becomes negative. The de Sitter mixing provides thus a natural explanation [64] for the anomalous results known as 'negative mass squared problem' for $\overline{\nu}_e$ [68].

The difference in mass squares

$$\Delta m^2 = \frac{\hbar^2}{c^2 r_0^2} \tag{4.10}$$

is independent of whether we evaluate it for the right, or left-handed fields. However, this is a frame-dependent evaluation. The rest frame of the interaction vertex defines the preferred frame of the calculation [63].

Identifying ρ_0 with an gravito-electroweak unification scale $M_{\rm unif}$ and using (4.3), we get

$$\Delta m^2 = \frac{8\pi}{3}\left(\frac{M_{\rm unif}}{m_{\rm Pl}}\right)^4 m_{\rm Pl}^2, \tag{4.11}$$

which connects mass-squared difference with the unification scale. So, when the mass-squared differences of neutrinos arise from the de Sitter mixing, the unification scale is immediately read off from (4.11) as [63, 64]

$$M_{\rm unif} = \left[\frac{3}{8\pi}\left(\frac{\Delta m^2}{m_{\rm Pl}^2}\right)\right]^{1/4} m_{\rm Pl}. \tag{4.12}$$

The atmospheric neutrino data [69]

$$\delta m^2_{\rm ATM} = 2.5 \times 10^{-3}\ {\rm eV}^2 \tag{4.13}$$

give for the unification scale

$$M_{\rm unif} \simeq 14.5\ {\rm TeV} \tag{4.14}$$

and mass-squared difference from solar neutrino data

$$\delta m^2_{\rm ATM} = 2.5 \times 10^{-3}\ {\rm eV}^2 \tag{4.15}$$

gives

$$M_{\rm unif} \simeq 5.9\ {\rm TeV}. \tag{4.16}$$

These correspond, respectively, to $r_0 = 0.4 \times 10^{-3}$ cm and $r_0 = 2.3 \times 10^{-3}$ cm, and justifies accuracy of calculations: for a particle with mass $\langle m\rangle_{\nu_e} = 0.39$ eV, characteristic curvature size is $r_s \sim 10^{-23}$ cm and Compton size $\lambda_C \sim 10^{-5}$ cm.

Assuming that a neutrino mass is essentially related to de Sitter group, we obtained estimates for the gravito-electroweak unification scale from neutrino experimental data [64], at the same scale as predicted by theories of gravito-electroweak unification [70].

4.2. Estimates on sizes of leptons

Electromagnetic and electro-weak experimental upper limits on sizes of leptons (see references in [65]) are much less than their Compton wavelength. This suggests that an extended fundamental particle can have relatively small characteristic geometrical size related to gravity.

We can estimate it by characteristic length scale r_* in geometry with the interior de Sitter vacuum. This implies rather natural assumption that whichever would be particular mechanism involving de Sitter vacuum in mass generation, a fundamental particle may have an internal vacuum core related to its mass and a geometrical size defined by gravity.

Geometrical size of an object with the interior de Sitter vacuum r_* depends on vacuum density at $r = 0$ and represents a modification of the Schwarzschild radius r_g to the case when singularity is replaced with the de Sitter vacuum. The resulting difference in sizes is quite impressive: for elementary particles the Schwarzschild radius is many orders of magnitude less than $l_{\rm Pl}$ (e.g., $r_g \sim 10^{-57}$ cm for the electron); the characteristic radius r_* gives values close to experimental upper limits, $r_* \sim r_{\rm exp} \sim 10^{-18}$ cm for the electron getting its mass from the vacuum at the electroweak scale [65].

We estimate geometrical sizes of fundamental particles by characteristic geometrical size given by curvature radius r_s (figure 4). In figure 6 [65] they are plotted by dark triangles, and compared with electromagnetic (EM) and electroweak (EW) experimental limits.

Geometrical sizes for leptons are calculated with using the density profile (2.6), but the results would not change drastically for different profiles, since a characteristic length scale in geometry with de Sitter interior is $r_* \sim \left(r_0^2 r_g\right)^{1/3}$ [22].

In figure 6 we show by stars quantum limits given by Compton wave length, by white triangles electromagnetic experimental upper limits coming mainly from reaction $e^+e^- \to \gamma\gamma(\gamma)$ [71], by shaded squares experimental electro-weak limits [72], by dark triangles geometrical limits on sizes calculated from (2.9) with ρ_0 of the electro-weak scale 246 GeV, and by dark squares the most stringent lower limits on sizes of particles as extended objects. This last limit is calculated by taking into account that in the case when de Sitter vacuum is involved in mass generation, quantum region of a particle localization λ_C must fit within a causally connected region confined by the de Sitter horizon r_0.

The requirement $\lambda_C \leqslant r_0$ gives the limiting scale for a vacuum density ρ_0 related to a given mass m [65]

$$\rho_0 \leqslant \frac{3}{8\pi}\left(\frac{m}{m_{\rm Pl}}\right)^2 \rho_{\rm Pl}. \tag{4.17}$$

This condition connects a mass of a quantum object m with the scale for vacuum density ρ_0 at which this mass could be generated in principle provided that a mechanism of generation involves de Sitter vacuum.

Let us compare characteristic sizes for an electron, its Compton wavelength, classical and Schwarzschild radius, with geometrical limits on lepton sizes for the case when de Sitter vacuum is involved on the electro-weak scale, on gravito-electroweak scale (4.16), and at the most stringent scale (4.17)

$$\lambda_C \simeq 3.9 \times 10^{-11}\ \text{cm}, \qquad r_{\rm em} \simeq 2.8 \times 10^{-13}\ \text{cm}, \qquad r_{\rm EW} \simeq 1.5 \times 10^{-18}\ \text{cm},$$
$$r_{\rm GEW} \simeq 2 \times 10^{-23}\ \text{cm}, \qquad r_{\rm lowest} \simeq 5 \times 10^{-26}\ \text{cm}, \qquad r_g \simeq 10^{-57}\ \text{cm}.$$

The numbers given by the de Sitter–Schwarzschild geometry are much bigger that the Planck scale $l_{\rm Pl} \sim 10^{-33}$ cm, which justifies application of classical general relativity for estimation of sizes of quantum particles.

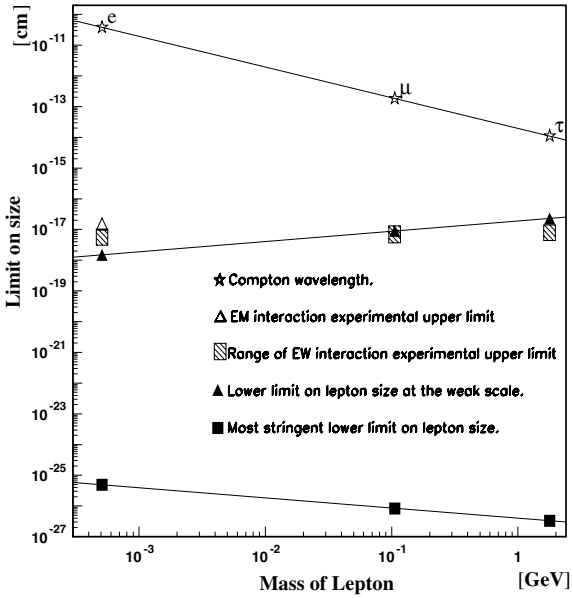

Figure 6. Characteristic sizes for leptons [65].

5. Summary

Nonlinear electrodynamics coupled to gravity suggests that spinning particles dominated by the electromagnetic interaction would have to have de Sitter interiors arising naturally in the regular geometry asymptotically Kerr–Newman for a distant observer.

In nonlinear electrodynamics coupled to gravity and satisfying the weak energy condition, regular spherically symmetric electrically charged structures have obligatory de Sitter center where the electric field vanishes while the electrovacuum energy density achieves its maximal value which gives an effective cut-off on self-energy density related to interior de Sitter vacuum $\Lambda = \kappa\rho_0$. Electromagnetic mass of spherical electrovacuum solitons is related to both de Sitter vacuum trapped inside and smooth breaking of spacetime symmetry from the de Sitter group in the origin to the Poincaré group at infinity.

By the Gürsey–Gürses algorithm they are transformed into spinning electrovacuum solitons, with the following generic behavior (found for an arbitrary nonlinear Lagrangian $\mathcal{L}(F)$):

(1) Kerr–Newman behavior for a distant observer.
(2) De Sitter vacuum spread over equatorial disk which
  (i) provides a finite cutoff on self-interaction,
  (ii) behaves as perfect conductor and ideal diamagnetic,
  (iii) supplies a particle with the finite electromagnetic mass related to breaking of spacetime symmetry.
(3) In this economic picture the interior rotating de Sitter vacuum disk displays superconducting behavior within a single spinning particle.

Applying these results to estimate the gravito-electroweak unification scale by the experimental data on neutrino mass-square difference, we read off the unification scale from

the solar and atmospheric neutrino data which gives $M_{\rm unif} \sim (6-15)$ TeV, i.e., at the same scale as predicted by theories of gravito-electroweak unification.

Estimating lepton sizes by characteristic gravitational scale for spacetime with interior de Sitter vacuum we obtain the reasonable numbers in agreement with the experimental limits.

Acknowledgment

This work was supported by the Polish Ministry of Science and Information Society Technologies through the grant 1P03D.023.27.

References

[1] Dymnikova I 1992 *Gen. Rel. Grav.* **24** 235
Dymnikova I 1990 CAMK *Preprint* 216
[2] Dymnikova I G 2000 *Phys. Lett.* B **472** 33
[3] Dymnikova I and Galaktionov E 2007 *Phys. Lett.* B **645** 358
[4] Dymnikova I 2002 *Class. Quantum Grav.* **19** 725
[5] Dymnikova I 2003 *Int. J. Mod. Phys.* D **12** 1015
[6] Dymnikova I 2006 *Phys. Lett.* B **639** 368
[7] Gliner E B 1966 *Sov. Phys.—JETP* **22** 378
[8] DeWitt B S 1967 *Phys. Rev.* **160** 1113
[9] Landau L D and Lifshitz E M 1975 *Classical Theory of Fields* (Oxford: Pergamon)
[10] Dymnikova I and Galaktionov E 2005 *Class. Quantum Grav.* **22** 2331
[11] Dymnikova I G, Dobosz A, Filchenkov M L and Gromov A A 2001 *Phys. Lett.* B **506** 351
[12] Bronnikov K A, Dobosz A and Dymnikova I G 2003 *Class. Quantum Grav.* **20** 3797
[13] Dymnikova I 2004 *Beyond the Desert 2003* ed H V Klapdor-Kleinhaus (Berlin: Springer) p 521
[14] Dymnikova I and Soltysek B 1998 *Gen. Rel. Grav.* **30** 1775
Dymnikova I and Soltysek B 1998 *Particles, Fields and Gravitation AIP Conf. Proc.* ed J Rembielinsky p 453
[15] Dymnikova I 2002 *Gravitation and Cosmology* **8** 131 (*Preprint* gr-qc/0201058)
[16] Dymnikova I G 1996 *Int. J. Mod. Phys.* D **5** 529
[17] Dymnikova I 1997 *Internal Structure of Black Holes and Spacetime Singularities* ed L M Burko and A Ori (*Ann. Isr. Phys. Soc.* vol 13) p 422
[18] Dymnikova I 2000 *Woprosy Matematicheskoj Fiziki i Prikladnoj Matematiki* ed E Tropp (St. Petersburg) p 29 (*Preprint* gr-qc/0010016)
[19] Dymnikova I 2002 *Gravitation and Cosmology* **8** 37
[20] Dymnikova I 2002 *General Relativity, Cosmology and Gravitational Lensing* ed G Marmo, C Rubano and P Scudellaro (Napoli: Bibliopolis) p 95
[21] Dymnikova I 2004 *Beyond the Desert 2003* ed H V Klapdor-Kleinhaus (Berlin: Springer) p 485
[22] Poisson E and Israel W 1988 *Class. Quantum Grav.* **5** L201
[23] Markov M A 1982 *JETP Lett.* **36** 265
Markov M A 1984 *Ann. Phys.* **155** 333
[24] Bernstein M R 1984 *Bull. Am. Phys. Soc.* **16** 1016
[25] Farhi E and Guth A 1987 *Phys. Lett.* B **183** 149
[26] Shen W and Zhu S 1988 *Phys. Lett.* A **126** 229
[27] Frolov V P, Markov M A and Mukhanov V F 1990 *Phys. Rev.* D **41** 3831
[28] Morgan D 1991 *Phys. Rev.* D **43** 3144
[29] Strominger A 1992 *Phys. Rev.* D **46** 4396
[30] Chapline G, Hohlfeld E, Laughlin R B and Santiago D I 2000 *Preprint* gr-qc/0012094
[31] Mazur P O and Mottola E 2001 *Preprints* gr-qc/0109035
Mazur P O and Mottola E 2001 *Preprints* gr-qc/0405111
Mazur P O and Mottola E 2004 *Proc. Nat. Acad. Sci.* **111** 9545
[32] Dymnikova I 2004 *Class. Quantum Grav.* **21** 4417
[33] Kaup D J 1968 *Phys. Rev.* **172** 1331
Ruffini R and Bonazzola S 1969 *Phys. Rev.* **187** 1767
[34] Mielke E W and Schunk F E 2000 *Nucl. Phys.* B **564** 185
[35] Gibbons G W and Hawking S W 1977 *Phys. Rev.* D **15** 2738
[36] Newman E T, Cough E, Chinnapared K, Exton A, Prakash A and Torrence R 1965 *J. Math. Phys.* **6** 918

[37] Carter B 1968 *Phys. Rev.* **174** 1559
[38] Chandrasekhar S 1983 *The Mathematical Theory of Black Holes* (Oxford: Clarendon)
[39] Israel W 1970 *Phys. Rev.* D **2** 641
[40] Burinskii A Ya 1974 *Sov. Phys.—JETP* **39** 193
[41] Hamity V H 1976 *Phys. Lett.* **56A** 77
[42] Krasinski A 1978 *Ann. Phys., NY* **112** 22
[43] López C A 1983 *Nuovo Cimento* **76B** 9
[44] Cohen J M and Cohen M D 1969 *Nuovo Cimento* **60** 241
[45] de la Cruz V, Chase J E and Israel W 1970 *Phys. Rev. Lett.* **24** 423
[46] Lopez C A 1984 *Phys. Rev.* D **30** 313
[47] Boyer R H 1965 *Proc. Camb. Phil. Soc.* **61** 527
Boyer R H 1966 *Proc. Camb. Phil. Soc.* **62** 495
[48] Trümper M 1967 *Z. Naturforsch.* **22a** 1347
[49] Tiomno J 1973 *Phys. Rev.* D **7** 992
[50] Tiwari R N, Rao J R and Kanakamedala R R 1984 *Phys. Rev.* D **30** 489
[51] Burinskii A Ya 1989 *Phys. Lett.* B **216** 123
[52] Burinskii A 2000 Supersymmetric superconducting bag as a core of Kerr spinning particle *Preprint* hep-th/0008129
[53] Burinskii A, Elizalde E, Hildebrandt S R and Magli G 2002 *Phys. Rev.* D **65** 064039 (*Preprint* gr-qc/0109085)
[54] Burinskii A 2005 *Preprint* hep-th/0506006
[55] Bronnikov K A 2001 *Phys. Rev.* D **63** 044005
[56] Kerr R P and Schild A 1964 *Am. Math. Soc. Symp.* (New York)
[57] Gurses M and Gursey F 1975 *J. Math. Phys.* **16** 2385
[58] Elizalde E and Hildebrandt S R 2002 *Phys. Rev.* D **65** 124024 (*Preprint* gr-qc/0202102)
[59] Landau L D and Lifshitz E M 1960 *Electrodynamics of Continued Media* (Oxford: Pergamon)
[60] Born M and Infeld L 1934 *Proc. R. Soc. Lond.* A **43** 410
Born M and Infeld L 1934 *Proc. R. Soc. Lond.* A **144** 425
[61] Seiberg N and Witten E 1999 *J. High Energy Phys.*JHEP09(1999)032 (*Preprint* hep-th/9908142)
[62] Fradkin E S and Tseytlin A 1985 *Phys. Lett.* B **163** 123
Tseytlin A 1985 *Nucl. Phys.* B **276** 391
[63] Ahluwalia D V and Dymnikova I 2003 *Preprint* hep-ph/0305158
[64] Ahluwalia-Khalilova D V and Dymnikova I 2003 *Int. J. Mod. Phys.* D **12** 1787
[65] Dymnikova I, Hasan A, Ulbricht J and Zhao J 2001 *Grav. Cosmol.* **7** 122
Dymnikova I, Ulbricht J and Zhao J 2001 *Quantum Electrodynamics and Physics of the Vacuum* ed G Cantatore (New York: AIP) p 239
[66] Dymnikova I 2008 *Nonlinear Electrodynamics in Gravitation Astrophysics and Cosmology* ed H J Mosquera Cuesta
[67] Gürsey F 1964 Group Theoretical concepts and methods in elementary particle physics *Lectures of the Istanbul Summer School in Theoretical Physics* ed F Gürsey (New York: Gordon and Breach)
[68] Stoeffl W and Decman D J 1995 *Phys. Rev. Lett.* **75** 3237
Stephenson G J Jr and Goldman T 1998 *Phys. Lett.* B **440** 89
Ciborowski J and Rembielinski J 1999 *Eur. Phys. J.* C **8** 157
Ehrlich R 1999 *Phys. Rev.* D **60** 017302
Ehrlich R 2000 *Phys. lett.* B **493** 229
[69] Pakvasa S and Valle J W F 2003 *Preprint* hep-ph/0301061
[70] Antoniadis I 1990 *Phys. Lett.* B **246** 377
Dvali G and Smirnov A Yu 1999 *Nucl Phys.* B **563** 63
Arkani-Hamed N *et al* 2000 *Phys. Rev. Lett.* **84** 586
[71] Acciari M *et al* (L3 Collaboration) 1996 *Phys. Lett.* B **384** 323
Acciari M *et al* (L3 Collaboration) 1997 *Phys. Lett.* B **413** 159
Acciari M *et al* (L3 Collaboration) 2000 *Phys. Lett.* B **475** 189
[72] Adloff C *et al* (HI Collaboration) 1997 *Nucl Phys.* B **483** 44
Derrick M *et al* (ZEUS Collaboration) 1995 *Z. Phys.* C **65** 627
Barate R *et al* (ALEPH Collaboration) 1998 CERN-EP/98-022
Mnich J *et al* (L3 Collaboration) 1999 *29th Int. Conf. High Energy Physics*